

# Revisiting the physiological roles of SGLTs and GLUTs using positron emission tomography in mice

Monica Sala-Rabanal<sup>1,5</sup>, Bruce A. Hirayama<sup>1</sup>, Chiara Ghezzi<sup>1</sup>, Jie Liu<sup>1</sup>, Sung-Cheng Huang<sup>1</sup>, Vladimir Kepe<sup>1,6</sup>, Hermann Koepsell<sup>2</sup>, Amy Yu<sup>1,7</sup>, David R. Powell<sup>3</sup>, Bernard Thorens<sup>4</sup>, Ernest M. Wright<sup>1</sup> and Jorge R. Barrio<sup>1</sup>

<sup>1</sup>The Department of Physiology and the Department of Molecular and Medical Pharmacology, David Geffen School of Medicine at UCLA, University of California, Los Angeles, CA, USA

<sup>2</sup>Julius-von-Sachs-Institute, Department of Molecular Plant Physiology and Biophysics, University of Würzburg, Würzburg, Germany

<sup>3</sup>Lexicon Pharmaceuticals, Inc., The Woodlands, TX, USA

<sup>4</sup>Centre for Integrative Genomics, University of Lausanne, Lausanne, Switzerland

<sup>5</sup>Present address: Department of Cell Biology and Physiology, and Center for the Investigation of Membrane Excitability Diseases, Washington University, Saint Louis, MO, USA

<sup>6</sup>Present address: Department of Nuclear Medicine, Cleveland Clinic, Cleveland, OH, USA

<sup>7</sup>Present address: Radiation Oncology, Stanford Hospital, Menlo Park, CA, USA

## Key points

- Glucose transporters are central players in glucose homeostasis.
- There are two major classes of glucose transporters in the body, the passive facilitative glucose transporters (GLUTs) and the secondary active sodium-coupled glucose transporters (SGLTs).
- In the present study, we report the use of a non-invasive imaging technique, positron emission tomography, in mice aiming to evaluate the role of GLUTs and SGLTs in controlling glucose distribution and utilization.
- We show that GLUTs are most significant for glucose uptake into the brain and liver, whereas SGLTs are important in glucose recovery in the kidney.
- This work provides further support for the use of SGLT imaging in the investigation of the role of SGLT transporters in human physiology and diseases such as diabetes and cancer.

**Abstract** The importance of sodium-coupled glucose transporters (SGLTs) and facilitative glucose transporters (GLUTs) in glucose homeostasis was studied in mice using fluorine-18 labelled glucose molecular imaging probes and non-invasive positron emission tomography (PET) imaging. The probes were:  $\alpha$ -methyl-4-[F-18]-fluoro-4-deoxy-D-glucopyranoside (Me-4FDG), a substrate for SGLTs; 4-deoxy-4-[F-18]-fluoro-D-glucose (4-FDG), a substrate for SGLTs and GLUTs; and 2-deoxy-2-[F-18]-fluoro-D-glucose (2-FDG), a substrate for GLUTs. These radio-labelled imaging probes were injected i.v. into wild-type, *Sglt1*<sup>-/-</sup>, *Sglt2*<sup>-/-</sup> and *Glut2*<sup>-/-</sup> mice and their dynamic whole-body distribution was determined using microPET. The distribution of 2-FDG was similar to that reported earlier (i.e. it accumulated in the brain, heart, liver and kidney, and was excreted into the urinary bladder). There was little change in the distribution of 2-FDG in *Glut2*<sup>-/-</sup> mice, apart from a reduction in the rate of uptake into liver. The major differences between Me-4FDG and 2-FDG were that Me-4FDG did not enter the brain and was not excreted into the urinary bladder. There was urinary excretion of Me-4FDG in *Sglt1*<sup>-/-</sup> and *Sglt2*<sup>-/-</sup> mice. However, Me-4FDG was not reabsorbed in the kidney in *Glut2*<sup>-/-</sup> mice. There were no differences in Me-4FDG uptake into the heart of wild-type, *Sglt1*<sup>-/-</sup> and *Sglt2*<sup>-/-</sup> mice. We conclude that GLUT2 is important in glucose liver transport and reabsorption of glucose in the kidney along with SGLT2 and SGLT1. Complete reabsorption of Me-4FDG from the glomerular filtrate in wild-type mice and the absence of reabsorption in the kidney in *Glut2*<sup>-/-</sup> mice confirm the importance of GLUT2 in glucose absorption across the proximal tubule.

(Resubmitted 7 January 2016; accepted after revision 17 March 2016; first published online 28 March 2016)

**Corresponding authors** Monica Sala-Rabanal, Department of Cell Biology and Physiology, Washington University, Saint Louis, MO 63110, USA. E-mail: msala@wustl.edu; and Ernest M. Wright, Department of Physiology, David Geffen School of Medicine at UCLA, Los Angeles, CA 90095, USA. E-mail: ewright@mednet.ucla.edu

**Abbreviations** CT, computed tomography; 2-FDG, 2-deoxy-2-[F-18]-fluoro-D-glucose; 4-FDG, 4-deoxy-4-[F-18]-fluoro-D-glucose; GLUT, facilitative glucose transporter;  $\alpha$ MDG, methyl-D-glucopyranoside; Me-4FDG,  $\alpha$ -methyl-4-[F-18]-fluoro-4-deoxy-D-glucopyranoside; PET, positron emission tomography; SGLT, sodium-dependent glucose transporter.

## Introduction

Glucose transporters are central to glucose homeostasis in the body. There are two major classes of transporters for transport into cells: the passive facilitated glucose transporters (GLUTs) (Mueckler & Thorens, 2013) and the active sodium-coupled glucose transporters (SGLTs) (Wright *et al.* 2011; Wright, 2013). The SGLTs couple inward glucose transport to the inward transport of sodium down the sodium electrochemical potential gradient across the cell membrane. Although the GLUTs are ubiquitously expressed throughout the body, it is generally considered that SGLTs are only expressed in the intestine to absorb glucose from food and in the kidney to reabsorb filtered glucose that would otherwise be lost in the urine. However, SGLT genes and proteins are expressed throughout the body (Nishimura & Naito, 2005; Chen *et al.* 2010; Vrhovac *et al.* 2015) and functional SGLTs are expressed in specific cells within the brain (Yu *et al.* 2010; Yu *et al.* 2013) and in cancer (Scafoglio *et al.* 2015). Their functional relevance in the body apart from that observed in the kidneys and intestine is yet to be determined.

The activity of GLUTs in animals and humans has been studied extensively using non-invasive positron emission tomography (PET) and the glucose analogue 2-deoxy-2-[F-18]-fluoro-D-glucose (2-FDG) (Phelps, 2004). In the present study, we have extended PET imaging to the SGLTs using two newly developed imaging probes,  $\alpha$ -methyl-4-[F-18]-fluoro-4-deoxy-D-glucopyranoside (Me-4FDG) and 4-deoxy-4-[F-18]-fluoro-D-glucose (4-FDG). As reported previously, 2-FDG is a high affinity substrate for GLUTs and a low affinity substrate for SGLTs. Me-4FDG is a high affinity substrate for SGLT1, a medium affinity substrate for SGLT2 and a very low affinity substrate for GLUTs. 4-FDG is a substrate for both GLUTs and SGLTs (Table 1) (Wright *et al.* 2011). 2-FDG accumulation in cells is based on its phosphorylation by hexokinase to its 6-phosphate, although neither Me-4FDG, nor 4-FDG are phosphorylated (Yu *et al.* 2010; Yu *et al.* 2013). 2-FDG is accumulated in cells after entry via GLUTs as a result of a metabolic sink effect, whereas Me-4FDG is only accumulated in cells expressing SGLTs via sodium cotransport. Me-4FDG is effectively trapped as a result of the low rate of exit via SGLTs and also because it is a poor substrate for GLUTs (Table 1).

We have explored the functional activity of SGLTs and GLUT2 in the body of conscious mice using Me-4FDG, 4-FDG and 2-FDG microPET imaging in wild-type mice, as well as in *Sglt1*<sup>-/-</sup>, *Sglt2*<sup>-/-</sup> and *Glut2*<sup>-/-</sup> mice. PET is a powerful non-invasive method with high spatial (3 mm<sup>3</sup>) and temporal (seconds) resolution for imaging the dynamic distribution of these fluorine-18 probes *in vivo*. Our results confirm that, *in vivo*, Me-4FDG is a poor substrate for GLUT1 or GLUT2; 4-FDG is a substrate for SGLTs and GLUTs; and 2-FDG is a poor substrate for SGLT1 and SGLT2 (Table 1). In the kidney, SGLT1 and 2 in series with GLUT2 are responsible for the bulk of glucose reabsorption of glucose from the glomerular filtrate. Under physiological conditions, SGLTs are the main pathway for glucose transport in the kidney and intestine, although our results suggest that, in other major organs, such as the brain, heart and liver, GLUTs are responsible for most of the glucose uptake. However, SGLT-mediated glucose utilization has been shown to be important in the brain (Yu *et al.* 2010) and in certain cancers (Scafoglio *et al.* 2015).

## Methods

### Animals

All animal procedures followed guidelines approved by the University of California Chancellor's Committee on Animal Research and the National Institutes of Health. We understand the ethical principles under which *The Journal of Physiology* operates and our work complies with the animal ethics policy and checklist as outlined recently (Grundy, 2015). Male and female wild-type C57Bl/6 mice (25–35 g; Jackson Laboratory, Bar Harbor, ME, USA), female *Glut2*<sup>-/-</sup> and male *Sglt1*<sup>-/-</sup> on a C57Bl/6-background, and male *Sglt2*<sup>-/-</sup> mice on a mixed 129S5/SvEvBrd x C57BL/6-Tyrc-Brd background (Thorens *et al.* 2000), (Gorboulev *et al.* 2012; Powell *et al.* 2013; Vallon, 2011) were housed at the UCLA Division of Laboratory Animal Medicine facilities and maintained under a 12:12 h light/dark cycle, with food and water available *ad libitum*. The *Sglt1*<sup>-/-</sup> mice were maintained on a low carbohydrate diet (Teklad TD08212; Harlan, Indianapolis, IN, USA) to avoid diarrhoea as a result of glucose-galactose-malabsorption (Wright *et al.* 2001;

**Table 1. Sugar selectivity of human SGLT1, SGLT2 and GLUT2**

	hSGLT1 $K_{0.5}$ (mM)	hSGLT2 $K_{0.5}$ or $K_i$ (mM)	hGLUT2 $K_{0.5}$ or $K_i$ (mM)
Glucose	0.5*	5 ( $K_{0.5}$ )***	~17 ( $K_{0.5}$ )****
2-FDG	>300**	34 ± 6 ( $K_i$ )	7 ± 2 ( $K_i$ )
4-FDG	0.1*	3 ± 1 ( $K_i$ )	14 ± 7 ( $K_i$ )
Me-4FDG	0.06 ± 0.02	16 ± 7 ( $K_i$ )	118 ± 40 ( $K_i$ )

The  $K_{0.5}$  value for Me-4FDG in hSGLT1 (mean ± SEM,  $n = 4$ ) and the  $K_i$  values for 2-FDG, 4-FDG and Me-4FDG in hSGLT2 and hGLUT2 (mean ± SEM,  $n = 3$  each) were estimated experimentally in the present study (Fig. 2), as described in the Methods. Other  $K_{0.5}$  values are taken from previous studies: \*Diez-Sampedro *et al.* (2001); \*\*Wright *et al.* (2011); \*\*\*Hummel *et al.* (2011); \*\*\*\*Mueckler & Thorens (2013). It is customarily assumed that the  $K_{0.5}$  and  $K_i$  parameters are interchangeable measures of transporter affinities for substrates.

Gorboulev *et al.* 2012). Some animals, as indicated in the text, were fasted overnight prior to each study, with free access to water, and studies were conducted between 10.00 h and 14.00 h. At the termination of experiments, animals were killed by terminal exsanguinations under deep isoflurane anaesthesia, followed by thoracotomy.

### Radiochemistry

2-FDG was obtained from the UCLA Cyclotron and Radiochemistry Technology Centre, and Me-4FDG and 4-FDG were synthesized from the corresponding acetylated galactose triflate by radiofluorination with cyclotron-produced [F-18]-fluoride, followed by deacetylation. Probes had high radiochemical purities of >97% and specific radioactivity >2,000 (Ci/mmol) (Wright *et al.* 2014).

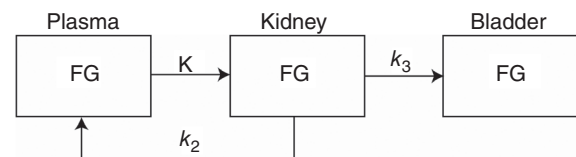
### In vivo microPET scanning

Experiments were performed at the Preclinical Imaging Technology Centre of the UCLA Crump Institute for Molecular Imaging. To determine the distribution of radiotracers in conscious mice, the protocol was to inject the tracer directly into the tail vein under isoflurane anaesthesia and, after recovery from the anaesthesia (<1 min), the animals were allowed to roam freely in their holding cage for 40 min before conducting a 10 min PET scan under anaesthesia, 50–60 min after injection of the tracer. Mice were anaesthetized in a heated induction box by inhalation of 2% isoflurane (Abbot Laboratories, North Chicago, IL, USA) in 100% oxygen. In mice subjected to 60 min dynamic PET scans, a small catheter (Intramedic PE20; Clay Adams, Sparks, MD, USA) was inserted in the proximal tail vein (Kreissl *et al.* 2011) and the tracer was injected after mounting the mouse on the

microPET scanner. The mice were positioned on a heated custom PET-CT small animal holder, which allowed for continuous anaesthesia (Suckow *et al.* 2009). A MicroPET Focus 220 scanner (CTI Concorde Microsystems, Knoxville, TN, USA) was used for PET data acquisition. For dynamic scans, the acquired data were binned into 25 image frames ( $3 \times 20$ ,  $4 \times 30$ ,  $5 \times 60$ ,  $5 \times 120$ ,  $3 \times 180$ ,  $3 \times 300$  and  $2 \times 600$  s). After the PET scans were completed, a 10 min computerized tomography (CT) scan was performed to provide anatomical information, using a MicroCAT II X-ray Tomograph (ImTek Inc., Knoxville, TN, USA). PET images were reconstructed using Fourier rebinning and a filtered back-projection algorithm (Kreissl *et al.* 2011; Wong *et al.* 2013) and microCT images were co-registered with microPET data for attenuation correction (Chow *et al.* 2005).

### Data analysis

AMIDE software (Loening & Gambhir, 2003) was used for image display and volume-of-interest analysis. Kinetic modelling of the excretion of 2-FDG or Me-4FDG into the urinary bladder was performed using the Kinetic Imaging System (Huang *et al.* 2005). The standard 2-FDG model was simplified to three compartments, plasma, kidney and bladder (Fig. 1), as a result of both 2-FDG and Me-4FDG being excreted into the urine unchanged (Gallagher *et al.* 1978; Yu *et al.* 2010). The rate constants describing tracer exchange between the three compartments are: (i)  $K$  ( $\text{ml min}^{-1}$ ), the clearance of tracer from plasma by the kidney by glomerular filtration; (ii)  $k_2$  ( $\text{min}^{-1}$ ), the reabsorption of tracer from the glomerular filtrate; and (iii)  $k_3$  ( $\text{min}^{-1}$ ), the rate of excretion of the tracer into the bladder from the kidney. It is also assumed that there is no secretion of 2-FDG or Me-4FDG from blood into the tubules (i.e.  $k_{-2}$  is zero) and there is no back-flow of tracer from the bladder into the kidney (i.e.  $k_{-4}$  is zero). If there is little or no reabsorption of tracer from the glomerular filtrate,  $k_2$  is zero, whereas, if there is little or no tracer excretion into the bladder,  $k_3$  would approach  $K$ . It is straightforward to measure the rate of tracer excretion into the bladder by following the whole bladder region of

**Figure 1. Kinetic model for urinary excretion of PET tracers**

Three-compartment model of urinary excretion of radiotracers (FG) from plasma. FG is the concentration of the radiotracer in plasma, kidney and urinary bladder.  $K$  is the rate of glomerular filtration,  $k_2$  is the rate of tubular reabsorption of filtered FG and  $k_3$  is the rate of excretion from the kidney into the urinary bladder.

interest, although it is problematic to measure the activity in plasma as a function of time, the input function (IF), because of the small blood volume in mice (Ferl *et al.* 2007; Kreissl *et al.* 2011; Wong *et al.* 2011). In the present study, we chose to estimate the input function by recording the activity in the heart and assuming that the total activity is within the heart chambers (total volume of 20  $\mu\text{l}$  in a 200–150 mg heart in a mouse weighing 27 g), and assuming a haematocrit of 50%. This is a reasonable first approximation because 2-FDG and Me-4FDG are not accumulated in the ventricular wall of the fasted mouse heart (see Results; see also Kreissl *et al.* 2011). Images were analysed using AMIDE where three dimensional ellipsoidal volumes were drawn over the region of interest (heart and bladder) on the PET image using the CT as an anatomic reference. There were no significant changes in the urinary bladder volume over the course of the 60 min microPET scans. The average radioactivity was calculated on each time frame to obtain the time course of the distribution in the heart and bladder. Each data point was converted to absolute radioactivity concentration ( $\text{MBq ml}^{-1}$ ) with the calibration factor derived from routine cylinder phantom experiments.

### In vivo metabolism of Me-4FDG

Me-4FDG, 4-FDG and 2-FDG were neither phosphorylated by hexokinase *in vitro*, nor metabolized in rats (Yu *et al.* 2010). In the present study, we tested whether or not Me-4FDG was metabolized in *Sgt1*<sup>-/-</sup> mice. Some 70 min after the injection of the probe into three *Sgt1*<sup>-/-</sup> mice for microPET/CT, blood (0.05 ml) and urine (0.1 ml) samples were collected. Plasma was extracted with three volumes of methanol and a sample analysed along with urine by radio-thin layer chromatography (silica gel thin layer chromatography plates, developed with 85% acetonitrile aqueous solution; read and quantitated by autoradiography); 98% and 91% of the [F-18] in plasma and urine ran as Me-4FDG.

### Probe selectivity

We examined the selectivity of 2-FDG, Me-4FDG and 4-FDG with respect to human SGLT1, SGLT2 and GLUT2 using transport assays in heterologous expression systems (Fig. 2 and Table 1). hSGLT1-mediated Me-4FDG transport was measured in *Xenopus laevis* oocytes expressing the transporter by means of two-electrode voltage clamp electrophysiology, and the apparent affinity constant  $K_{0.5}$  for Me-4FDG transport was determined by fitting the concentration-dependent  $\text{Na}^+$ /sugar currents to a Michaelis–Menten relationship, as described previously in studies from our laboratory (Diez-Sampedro *et al.* 2001). 2-FDG, 4-FDG and Me-4FDG interactions with hSGLT2 and hGLUT2 were determined by

competition assays in HEK293T cells transfected with the transporter cDNAs, as described previously (Hummel *et al.* 2011; Ghezzi *et al.* 2014). Briefly, the uptake of 50  $\mu\text{M}$  [C-14]-D- $\alpha$ -methyl-D-glucopyranoside (for hSGLT2; Moravsek Biochemicals, Brea, CA, USA) or 2 mM [C-14]-2-deoxy-D-glucose (for hGLUT2; PerkinElmer, Boston, MA, USA) was measured in the absence and presence of increasing concentrations of external 2-FDG, 4-FDG or Me-4FDG, and the results were corrected for uptake in untransfected cells. The apparent inhibitory constant  $K_i$  values were estimated from the relationship for competitive inhibition (eqn III-5 in Segel, 1975):

$$J = [I] / ([I] + K_i (1 + [S] / K_m)) \quad (1)$$

where  $J$  is the fractional inhibition of uptake at each concentration of inhibitor  $I$ ;  $S$  is the substrate concentration; and  $K_m$  is the apparent affinity of the sub-

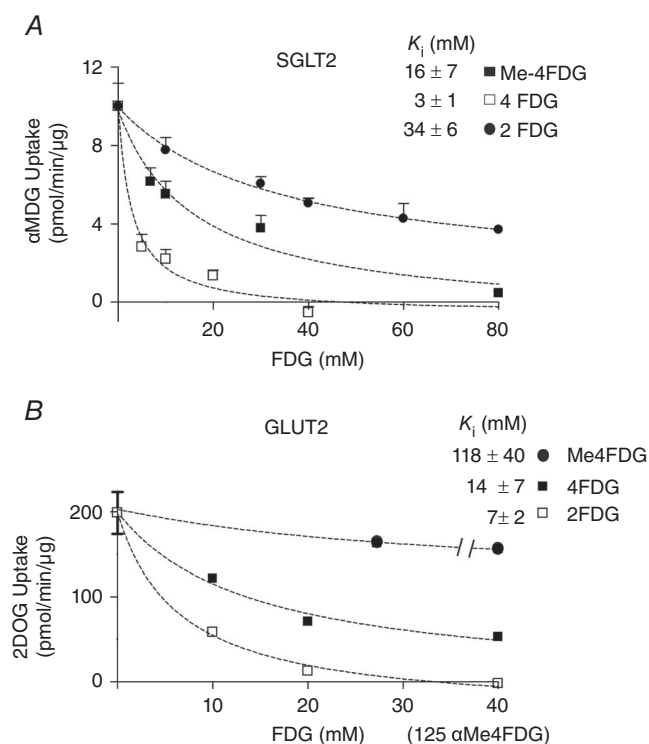


**Figure 2. Sugar selectivity of hSGLT2 and hGLUT2**

A, sugar  $K_i$  values for hSGLT2. [<sup>14</sup>C]  $\alpha$ MDG uptake was measured in HEK-293T cells expressing hSGLT2 at increasing concentrations of Me-4FDG (black squares), 4-FDG (white squares) and 2-FDG (black circles). Data were fitted to eqn (1) to estimate the apparent inhibitory constant ( $K_i$ ). Data are the mean  $\pm$  SEM ( $n \geq 4$ ). B, sugar  $K_i$  values for GLUT2 [<sup>14</sup>C] 2-Deoxy-D-glucose uptake was measured in HEK-293T cells expressing hGLUT2 at increasing concentrations of Me-4FDG (black circles), 4-FDG (black squares) and 2-FDG (white squares). The break in the Me-4FDG curve indicates a break in the Me-4FDG concentration to a maximum of 125 mM, as noted in parenthesis on the abscissa. Data were fitted to eqn (1) to estimate the apparent inhibitory constant ( $K_i$ ). Data points are the mean  $\pm$  SEM ( $n \geq 4$ ).



strate. The  $K_{0.5}$  value for Me-4FDG in hSGLT1 and the  $K_i$  values for 2-FDG, 4-FDG and Me-4FDG in hSGLT2 and hGLUT2 estimated experimentally in the present study are shown in Table 1, alongside other relevant  $K_{0.5}$  values from previous studies.

### Statistical analysis

SigmaPlot, version 10.0 (Systat Software, San Jose, CA, USA) and CorelDRAW X3, version 13.0 (Corel Corporation, Mountain View, CA, USA) were used for data analysis and figure preparation. Unless otherwise noted, data are shown as the mean  $\pm$  SEM of at least three experiments. Statistical analyses were performed with OriginLab (Northampton, MA, USA). For each tracer (Figs 3B, 4B and 5B), the differences in 60 min conscious uptake were examined in two independent sets. On the one hand, differences in tissue accumulation between mouse types were evaluated by means of two-way ANOVA followed by Tukey's test, using organ (brain, heart, muscle and kidney) and genotype (wild-type and *Sglt1*<sup>-/-</sup>, *Sglt2*<sup>-/-</sup> or *Glut2*<sup>-/-</sup>, as appropriate) as the independent variables; statistically significant differences ( $P < 0.05$ ) are indicated (Figs 3B, 4B and 5B, left). On the other hand, differences in tracer excretion into the urinary bladder between mouse types were investigated by means of one-way ANOVA and *post hoc* Tukey's test (Figs 3B, 4B and 5B, right;  $P < 0.05$  was considered statistically significant). Additionally, where indicated in the text, one-way ANOVA and the Tukey test were applied to examine differences between isotopes in certain organs and mouse genotypes; the significance values are given as appropriate.

### Results

As a prelude to our microPET/CT studies aiming to examine the distribution of the three molecular imaging glucose tracers in conscious wild-type mice and in mice lacking three different glucose transporter genes, *Sglt1*, *Sglt2* and *Glut2*, we completed experiments on the selectivity of the tracers for hSGLT2 and hGLUT2. Figure 2 shows competition for hSGLT2 methyl-D-glucopyranoside ( $\alpha$ MDG) uptake by 2-FDG, 4-FDG and Me-4FDG (Fig. 2A) and competition for hGLUT2 [C-14]-2-deoxy-D-glucose uptake by 2-FDG, 4-FDG and Me-4FDG (Fig. 2B). As summarized in Table 1 the  $K_{0.5}$  and  $K_i$  values show that Me-4FDG is specific for SGLTs; 2-FDG is fairly specific for GLUT2; and 4-FDG, is transported by both SGLTs and GLUTs. A major difference between 2-FDG and the other two glucose tracers is that, although 2-FDG converted by hexokinase within cells to 2-FDG-6-phosphate, neither Me-4FDG, nor 4-FDG are metabolized in rats (Yu *et al.* 2010). This means that 2-FDG is accumulated in cells by a metabolic sink affect, whereas Me-4FDG and 4-FDG are

accumulated through the activity of SGLTs. We measured the steady-state distribution (at 60 min) of the three tracers in conscious mice (static scans) and the time course of the distribution of the imaging tracers in anaesthetized mice (dynamic scans).

The present study aimed to locate the functional expression of SGLTs throughout the whole body of the mouse. The data are presented in three ways; the first shows volumetric images of the distribution of each glucose tracer at 60 min in conscious wild-type and knockout mice (Figs 3A to 5A); the second tabulates the accumulation of the tracer in each major organ of these conscious mice at 60 min post tracer injection in terms of the percentage of the injected dose per gramme of each organ (%ID/g) (Figs 3B to 5B); and the third presents the time course of tracer accumulation in the major organs under isoflurane anaesthesia (Figs 3 to 5C–G and 6).

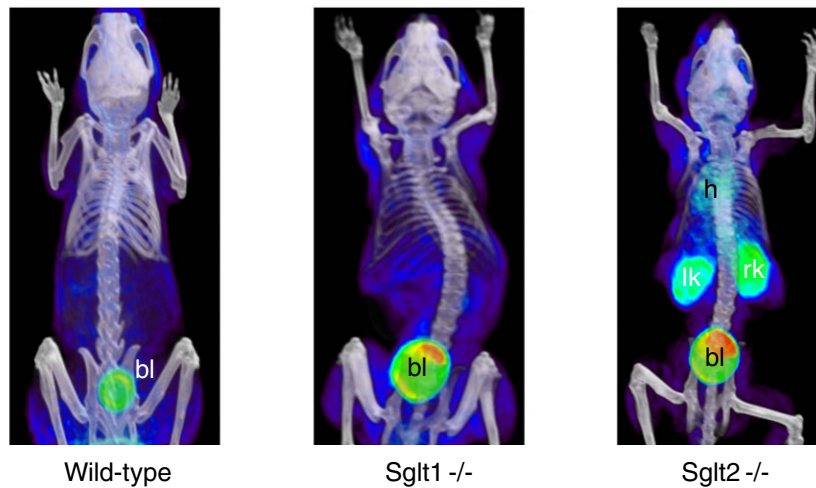
Pilot studies were conducted on fasted and non-fasted, conscious and anaesthetized and male and female mice. Where possible, at least two of the three tracers were compared on the same mice within 2 weeks. The distribution of 2-FDG and Me-4FDG in male, anaesthetized wild-type mice was similar in fasted and fed animals, except that 2-FDG was accumulated in the heart of fed but not fasted mice as reported previously (Kreissl *et al.* 2011). Similarly, there were no consistent changes in the distribution of 2-FDG, Me-4FDG and 4-FDG between conscious and anaesthetized fed mice (data not shown).

### Me-4FDG

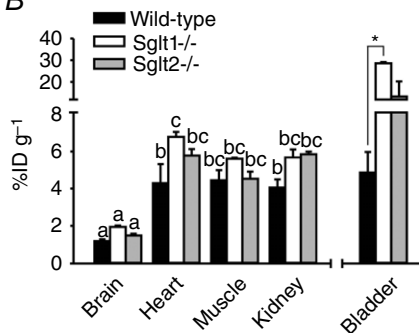
Immediately following i.v. injection of the tracer into the anaesthetized mouse and following blood flow, the [F-18] activity distributed to the major organs of the body. The blood activity then declined gradually as the tracer was taken up into tissues and excreted into the urine (Fig. 3C, D and F). Only in skeletal muscle was there clear evidence of a time-dependent slow accumulation of Me-4FDG (Fig. 3E), although there were no apparent differences in the time course between wild-type, *Sglt1*<sup>-/-</sup> and *Sglt2*<sup>-/-</sup> mice (Fig. 3E) and the 60 min uptake values ( $\sim$ 5%ID/g) were not significantly different (Fig. 3B). Me-4FDG was evenly distributed throughout wild-type mouse organs, except that there was almost no uptake into the brain (Fig. 3B). At 60 min, the percentage of the initial injected dose in heart, kidney and skeletal muscle was  $\sim$ 4%ID/g, which is significantly higher than for brain at 1%ID/g (Fig. 3B). The 60 min uptake into heart and kidney was higher for the *Sglt1* and *Sglt2* knockout animals (5–7 vs. 4%ID/g), although differences were only significant between the hearts of WT and *Sglt1*<sup>-/-</sup> mice. There was a very low excretion of Me-4FDG into the urinary bladder of wild-type mice and, as expected, this increased dramatically in the *Sglt1* and *Sglt2* knockout animals (Fig. 3B). This is discussed further below.

A

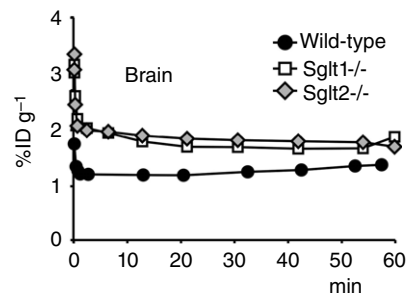
Me-4FDG



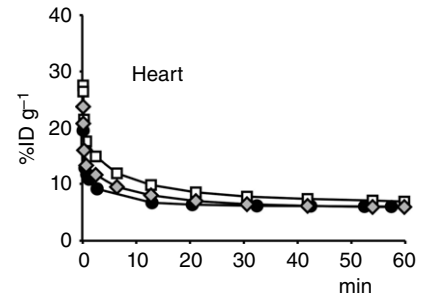
B



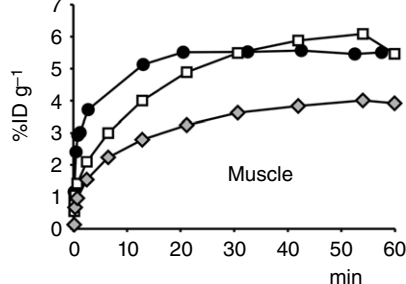
C



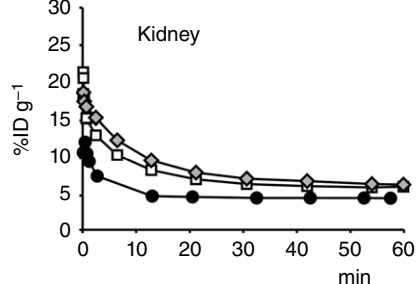
D



E



F



G

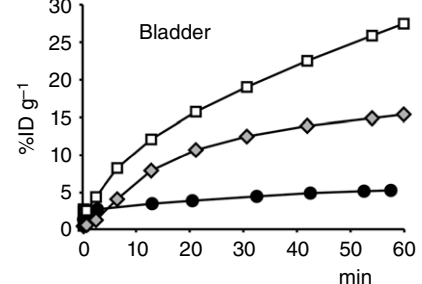


**Figure 3. Bio-distribution of novel SGLT-specific PET tracer Me-4FDG in mice**

A and B, non-metabolized glucose analogue Me-4FDG (300  $\mu$ Ci) was administered by tail vein injection into conscious wild-type, Sglt1<sup>-/-</sup> or Sglt2<sup>-/-</sup> mice and, after 40 min, the animals were anaesthetized for short PET/CT scans. A, volumetric renderings of representative co-registered scans; PET images are displayed according to the NIH intensity scale for tracer activity, from red (highest) to green (intermediate) to purple (lowest). Target organs are indicated: heart (h), urinary bladder (bl), left kidney (lk) and right kidney (rk). B, 60 min tracer activity detected in major target organs and tissues in conscious mice, as quantified by volume-of-interest (VOI) analysis for the experiments in (A); *Kidney* refers to the right kidney and *Muscle* refers to a 64 mm<sup>3</sup> spherical VOI from the inner right thigh (the same in all mice). Data are the mean  $\pm$  SEM of three to six experiments. Significant differences in tissue distribution (brain, heart, muscle and kidney) between wild-type, Sglt1<sup>-/-</sup> and Sglt2<sup>-/-</sup> mice are indicated by different lowercase letters ( $P < 0.05$ , two-way ANOVA and Tukey's test). Significant differences in excretion into the urinary bladder between mouse types are indicated by an asterisk ( $P < 0.05$ , one way ANOVA and Tukey's test). C–G, time-course of Me-4FDG distribution in unconscious mice. Tracer (300  $\mu$ Ci) was injected into anaesthetized animals, and continuous PET data were acquired for 60 min. For clarity, only select time points are represented. All data are from the same wild-type, Sglt1<sup>-/-</sup> or Sglt2<sup>-/-</sup> mouse, and are representative of at least three experiments in different mice.

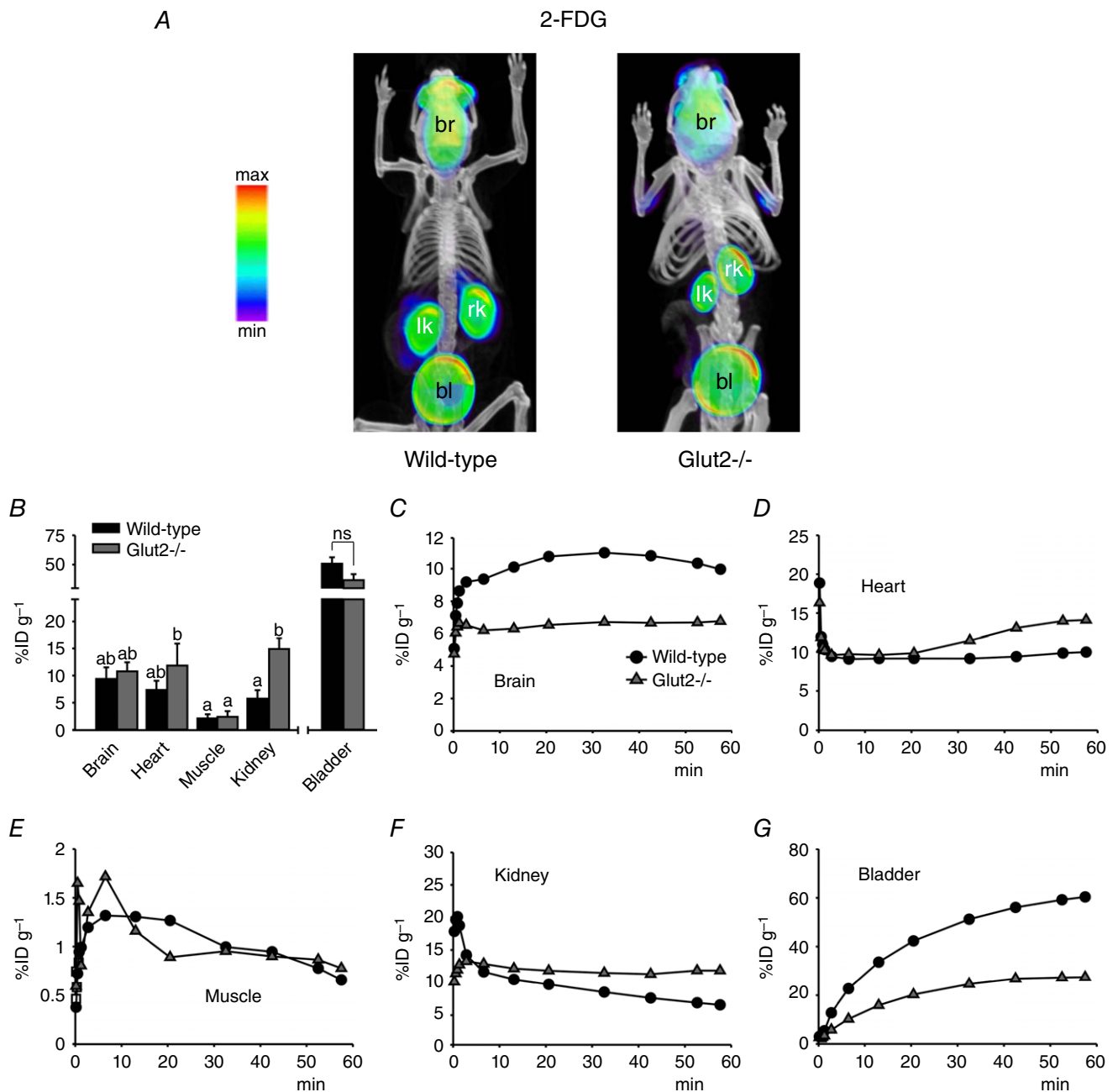


**Figure 4. Bio-distribution of GLUT-specific PET tracer 2-FDG in mice**  
 A and B, standard PET tracer 2-FDG (300  $\mu$ Ci) was administered by tail vein injection into conscious wild-type or Glut2<sup>-/-</sup> mice and, after 40 min, the animals were anaesthetized for short PET/CT scans. A, volumetric renderings of representative co-registered scans; PET images are displayed and labelled as in Fig. 3A. B, 60 min tracer activity detected in major target organs and tissues in conscious mice, as in Fig. 3B. Data are the mean  $\pm$  SEM of five to seven experiments. Significant differences in tissue distribution (brain, heart, muscle and kidney) between wild-type and Glut2-null mice are indicated by different lowercase letters ( $P < 0.05$ , two-way ANOVA and Tukey's test). Differences in excretion into the urinary bladder between mouse types were not significant (ns;  $P = 0.09$ , one-way ANOVA and Tukey's test). C–G, time-course of 2-FDG distribution in unconscious mice. Tracer (300  $\mu$ Ci) was injected into anaesthetized animals, and continuous PET data were acquired for 60 min. For clarity, only select time points are represented. All data are from the same wild-type or Glut2<sup>-/-</sup> mouse, and are representative of at least three experiments in different mice.

## 2-FDG

The 60 min distribution of 2-FDG in fasted wild-type conscious mice is very similar to that reported previously for anaesthetized mice (Landau *et al.* 2007; Wong *et al.* 2011). The most obvious differences between 2-FDG and Me-4FDG in wild-type animals were that 2-FDG accumulated in the brain (Figs 3B and C and 4B and C) and was excreted into the urinary bladder (Figs 3A, B and G and 4A, B and G). The 60 min accumulation of 2-FDG in the brain or excretion into the bladder (Fig. 3B) was significantly higher than that for Me-4FDG (Fig. 3B), respectively  $\sim 10$  vs.  $1\%$ ID/g and  $\sim 50$  vs.  $5\%$ ID/g ( $P < 0.01$  for both, one-way ANOVA and Tukey's test). There were no significant differences between wild-type and Glut2 knockout animals with respect to the average accumulation of 2-FDG in the brain, muscle and urinary bladder and, although tracer uptake in the heart was 60% higher in Glut2<sup>-/-</sup> than in wild-type mice, these differences were not statistically significant. On the other hand, there was a significant, 2.5-fold increase in 2-FDG uptake in the kidney of Glut2-null animals with respect to wild-type (Fig. 4B). In Glut2 knockouts, the slightly higher 60 min 2-FDG uptake in the heart is reflected in a slow accumulation of the tracer in tissue after the initial clearance of the vascular pool (Fig. 4D).

## 4-FDG

Unlike Me-4FDG, 4-FDG accumulated in the brain of wild-type mice (Figs 5B and C and 3B and C),  $\sim 4$  vs.  $1\%$ ID/g at 60 min ( $P < 0.01$ , one-way ANOVA and Tukey's test), and at levels comparable to those of 2-FDG (Figs 3B and C and 5B and C),  $\sim 4$  vs.  $10\%$ ID/g at 60 min ( $P = 0.15$ , one-way ANOVA and Tukey's test). This was expected given that 4-FDG is a substrate for both SGLTs and GLUTs, there is no metabolic sink for 4-FDG, and 4-FDG may exit the cell via GLUTs. The 60 min accumulation of 4-FDG in the muscle, heart and kidney of wild-type mice was similar in magnitude to that observed for Me-4FDG in wild-type mice and for 6-FDG (6-[F-18]-fluoro-6-deoxy-D-glucose) in rat (Landau *et al.* 2007). 6-FDG is a substrate for both SGLTs and GLUTs. Similar to 4-FDG, 6-FDG is not phosphorylated because it has no hydroxyl group at carbon-6. In Glut2 knockouts, there was a significantly higher accumulation of 4-FDG in the kidney with respect to wild-type (i.e.  $\sim 20$  vs.  $4\%$ ID/g at 60 min) (Fig. 5B), which may reflect a slower exit of 4-FDG accumulated through brush-border SGLTs. 4-FDG accumulated into brain and heart of Glut2-null mice was  $\sim 1.5$ - and  $\sim 2$ -fold higher than in the WT, respectively, and excretion into the urinary bladder was  $\sim 2.5$ -fold higher, although these differences were not found to be statistically significant (Fig. 5B).

## Tracer uptake into liver

The liver was of particular interest because this organ plays an important role in glucose homeostasis and GLUT2 is the major glucose transporter for hepatic glucose utilization (Guillam *et al.* 1998). The time course of 2-FDG accumulation in the liver of wild-type mice exhibited a rapid phase corresponding to early tissue uptake of the tracer followed by washout,  $t_{1/2} \sim 10$  min, to a 60 min level of  $5.0 \pm 0.2\%$ ID/g (Fig. 6). The difference in the time/activity curves for 2-FDG in wild-type and Glut2<sup>-/-</sup> mice reflects the importance of GLUT2-mediated 2-FDG uptake into liver. There were no differences in the Me-4FDG time/activity curves for wild-type, Sglt1<sup>-/-</sup> and Sglt2<sup>-/-</sup> mice (not shown), with 60 min distributions of  $6.0 \pm 0.4\%$ ID/g ( $n = 2$ ),  $6.0 \pm 0.2\%$ ID/g ( $n = 3$ ) and  $5.3 \pm 0.2\%$ ID/g ( $n = 5$ ), respectively. This indicates the absence of significant SGLT activity in liver.

## Urinary excretion

Striking differences were noted for the activities of the three glucose tracers in the urinary bladder of wild-type and knockout mice (Figs 3B, 4B and 5B). In terms of kidney function, it is desirable to express the activity as the total amount of tracer excreted into the bladder rather than the concentration in urine (Figs 3–5). The total amount of 2-FDG and Me-4FDG excreted into the urinary bladder (MBq) for representative wild-type, Sglt1<sup>-/-</sup>, Sglt2<sup>-/-</sup> and Glut2<sup>-/-</sup> mice is shown in Fig. 6. Note that these mice did not urinate during the experiments (i.e. no loss of activity from the animal) and so the amount in the bladder was an accurate reflection of the difference between the amounts of sugar tracer filtered and reabsorbed. It was previously reported that 2-FDG and Me-4FDG are excreted unchanged into urine (Gallagher *et al.* 1978; Yu *et al.* 2010). There was a low excretion of Me-4FDG into the urinary bladder of the wild-type mouse ( $<0.05$  MBq in 60 min), whereas 2-FDG excretion in wild-type and Glut2-null (not shown) mice increased rapidly after an initial delay of 1–2 min and approached a maximum of 2 MBq in 30 min: at 60 min, the amount of 2-FDG in the bladder was  $1.9 \pm 0.3$  MBq in wild-type mice ( $n = 3$ ) and  $2.5 \pm 0.3$  MBq in Glut2<sup>-/-</sup> mice ( $n = 2$ ).

The excretion of Me-4FDG in the Glut2<sup>-/-</sup> mouse followed a similar time course and magnitude to that observed for 2-FDG (Fig. 7). The rate and magnitude of Me-4FDG excretion in the Sglt1<sup>-/-</sup> and Sglt2<sup>-/-</sup> mice were intermediate between those observed for wild-type and Glut2<sup>-/-</sup> mice (Fig. 7). At 60 min, the bladder activity of Me-4FDG in Sglt1<sup>-/-</sup> or Sglt2<sup>-/-</sup> mice,  $1.3 \pm 0.1$  MBq ( $n = 3$ ) and  $1.2 \pm 0.9$  MBq ( $n = 6$ ), respectively, was significantly higher than in wild-type mice,  $0.05 \pm 0.03$  MBq ( $n = 5$ ) ( $P < 0.05$ , one-way



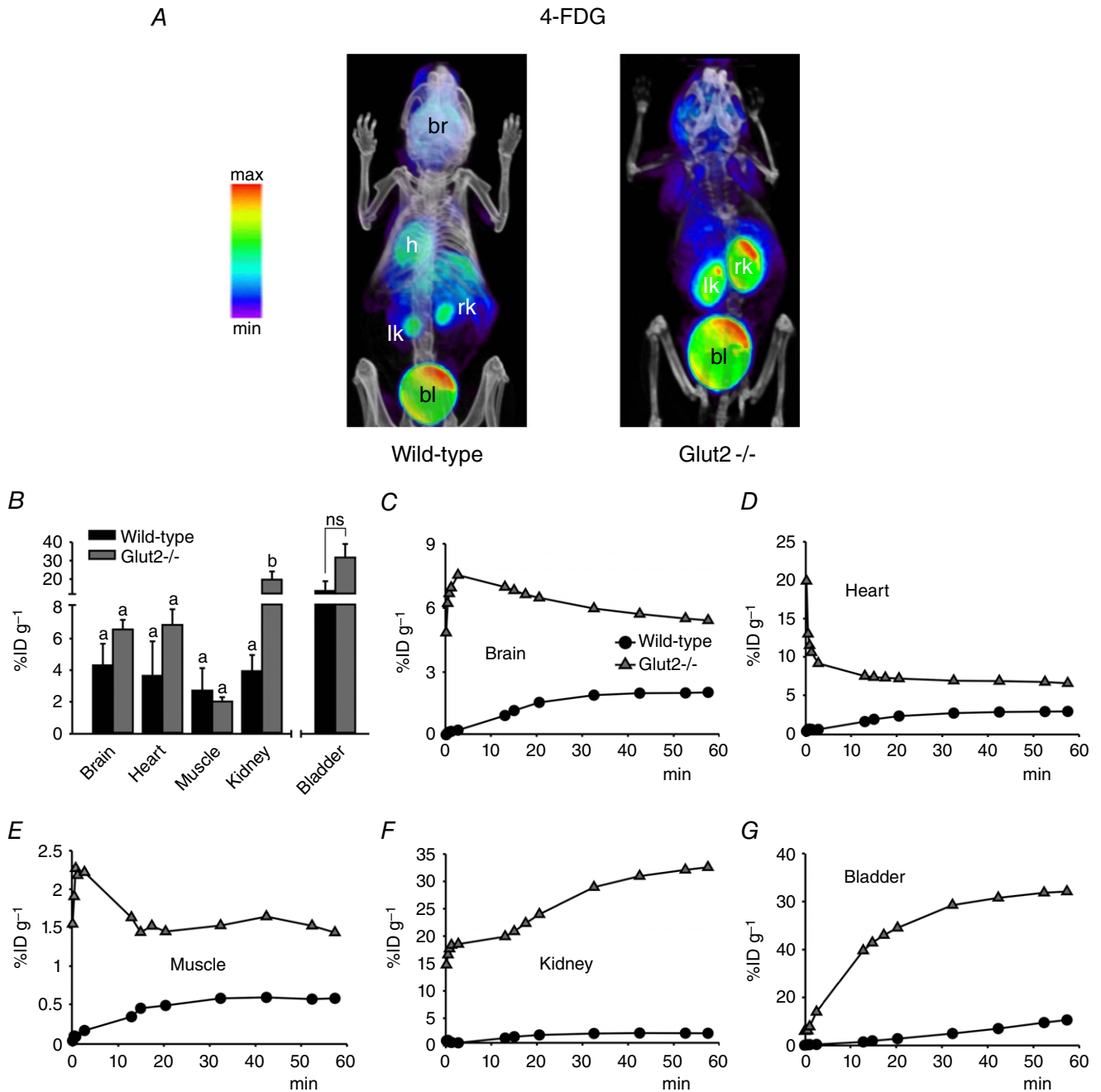


**Figure 5. Bio-distribution of novel glucose PET tracer 4-FDG in mice**  
 A and B, 4-FDG (300  $\mu$ Ci) was administered by tail vein injection into conscious wild-type or Glut2<sup>-/-</sup> mice and, after 40 min, the animals were anaesthetized for short PET/CT scans. A, volumetric renderings of representative co-registered scans; PET images are displayed and labelled as in Fig. 3A. B, 60 min tracer activity detected in major target organs and tissues in conscious mice, as in Fig. 3B. Data are the mean  $\pm$  SEM of three to six experiments. Significant differences in tissue distribution (brain, heart, muscle and kidney) between wild-type and Glut2-null mice are indicated by different letters ( $P < 0.05$ , two-way ANOVA and Tukey's test). Differences in excretion into the urinary bladder between mouse types were not significant (ns;  $P = 0.1$ , one-way ANOVA and Tukey's test). C–G, time-course of 4-FDG distribution in unconscious mice. Tracer (300  $\mu$ Ci) was injected into anaesthetized animals, and continuous PET data were acquired for 60 min. For clarity, only select time points are represented. All data are from the same wild-type or Glut2<sup>-/-</sup> mouse, and are representative of at least three experiments in different mice.

ANOVA and Tukey's test). Kinetic modelling of the rates of 2-FDG and Me-4FDG excretion shown in Fig. 6 provides an approximate estimate of glomerular filtration rate ( $K_1$ ) and the rate of glucose tracer reabsorption (Fig. 1). Uncertainty is a result of the indirect method required to estimate the input function (IF; plasma tracer concentration as a function of time after i.v. injection). Nevertheless, fits to the urinary excretion data (Fig. 7) give glomerular filtration rates of between 60 and 120  $\mu\text{l min}^{-1}$ ,

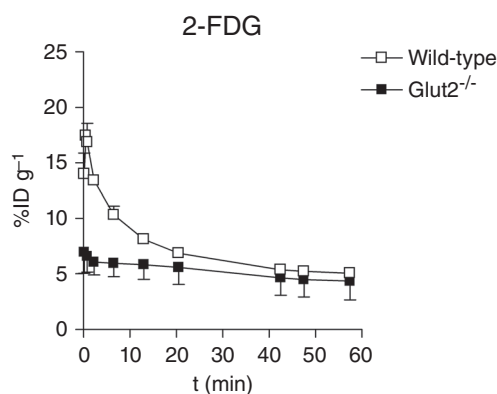


**Figure 6. Time course of 2-FDG distribution in the liver of wild-type and  $\text{Glut2}^{-/-}$  mice**

2-FDG (300  $\mu\text{Ci}$ ) was administered by tail vein into anaesthetized wild-type and  $\text{Glut2}^{-/-}$  mice and the activity in the right lobe of the liver was monitored for 60 min as in the experiments shown in Figs 3–5. Data are the mean  $\pm$  SEM for three wild-type and three  $\text{Glut2}^{-/-}$  mice.

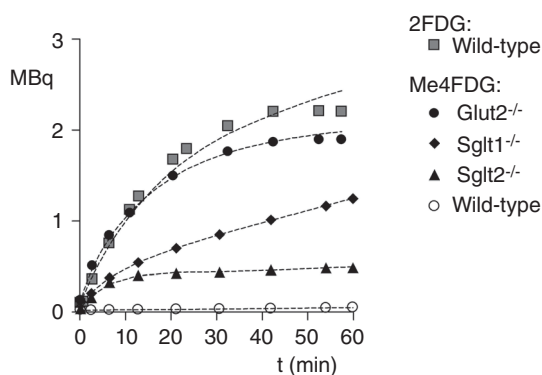


**Figure 7. Urinary excretion of PET tracers 2-FDG and Me-4FDG in wild-type,  $\text{Glut2}^{-/-}$ ,  $\text{Sglt1}^{-/-}$  and  $\text{Sglt2}^{-/-}$  mice**

The total amount of 2-FDG and Me-4FDG in the urinary bladder of representative WT,  $\text{Sglt1}^{-/-}$ ,  $\text{Sglt2}^{-/-}$  and  $\text{Glut2}^{-/-}$  mice as a function of time after i.v. injection of radiotracer (11 MBq) is shown. The data were fit to a three-compartment model (Fig. 1) using the Kinetic Imaging System (Huang *et al.* 2005). Fits to the urinary excretion data give glomerular filtration rates between 60 and 120  $\mu\text{l min}^{-1}$ . Estimates of the rate of tubular reabsorption ( $k_2$ ) for Me-4FDG were 0.23  $\pm$  0.26 for WT, 0.060  $\pm$  0.03 for  $\text{Sglt1}^{-/-}$ , 0.09  $\pm$  0.01 for  $\text{Sglt2}^{-/-}$  and 0.02  $\pm$  0.003 for  $\text{Glut2}^{-/-}$ ; estimates for 2-FDG were 0.03  $\pm$  0.01 for WT and 0.03  $\pm$  0.02 for  $\text{Glut2}^{-/-}$  (time-course not shown). The large error for the estimate of  $k_2$  for the wild-type mouse is a result of the low level of excretion.

which are comparable to estimates based on plasma clearance kinetics of fluorescein isothiocyanate-insulin (200–300  $\mu\text{l min}^{-1}$ ) (Vallon *et al.* 2010; Vallon, 2011; Powell *et al.* 2013). Modelling also provides estimates of the rates of Me-4FDG reabsorption in the range from 0.3  $\text{min}^{-1}$  for wild-type to 0.02  $\text{min}^{-1}$  for the  $\text{Glut2}$  knockout animal. The low rate of reabsorption of Me-4FDG for the  $\text{Glut2}$  knockout was similar to that for 2-FDG in both wild-type and knockout mice, suggesting an important role of basolateral GLUT2 in sugar reabsorption. The rates of Me-4FDG reabsorption in  $\text{Sglt1}^{-/-}$  and  $\text{Sglt2}^{-/-}$  mice were intermediate between Me-4FDG and 2-FDG in wild-type mice (i.e. 100%, 40% and 25% of the Me-4FDG filtered load was absorbed in 1 h in wild-type,  $\text{Sglt1}^{-/-}$  and  $\text{Sglt2}^{-/-}$  mice).

## Discussion

Glucose homeostasis involves complex relationships between glucose input (diet and gluconeogenesis in the liver and kidney), exchange between blood and tissues, metabolism, and excretion by the kidneys. In glucose exchange between blood and tissues, attention has focused almost exclusively on plasma membrane GLUTs. Another class of transporters, the SGLTs, are expressed in the small intestine and kidney and are largely responsible for intestinal glucose absorption from food in the small intestine (SGLT1) and glucose reabsorption from the glomerular filtrate in the kidney (SGLT2 and SGLT1) (Wright *et al.* 2011). Although SGLT proteins are known to be expressed and functional in other organs (e.g. the brain) (Yu *et al.* 2010; Yu *et al.* 2013), relatively little is known about their physiological importance *in vivo*. A powerful non-invasive method, 2-FDG PET, has been developed to study glucose distribution in the whole body of animals and humans. 2-FDG is taken up into cells through GLUTs in the plasma membrane and is trapped intracellularly by conversion to 2-FDG-6-phosphate, which is not a substrate for GLUTs. As a result, 2-FDG PET imaging is used for experimental and clinical studies to monitor glucose uptake into normal cells and tumours in the body (Phelps, 2004).

The advantages of PET are that it is a non-invasive method, which enables several experiments to be conducted on the same subject over time as a result of the short half-life of [F-18] (110 min), and the images of the [F-18] tracer distribution are obtained with high temporal and spatial resolution. Although the spatial resolution is high (3  $\text{mm}^3$ ), this does pose a limitation in mice when a limited number of cells in a small organ express glucose transporters, as revealed, for example, by the immunohistochemical location of SGLT1 in liver bile ducts (Balen *et al.* 2008; Vrhovac *et al.* 2015).

2-FDG is a poor substrate for SGLTs (Table 1) and, as a result, 2-FDG PET does not report accurately on SGLT

activity in the body. Although SGLT2 has a low affinity for 2-FDG, this does not appear to be relevant physiologically because little 2-FDG is reabsorbed in the proximal tubule (i.e. <10% of the filtered 2-FDG load is absorbed) (Fig. 6).

As expected, the whole distribution of 2-FDG in the anaesthetized, fasted control mice was similar to that reported previously (i.e. 2-FDG was accumulated in the brain, heart, and kidney, and was avidly excreted into the urinary bladder, whereas there was low accumulation in skeletal muscle) (Landau *et al.* 2007; Wong *et al.* 2011). There was no dramatic change in 2-FDG distribution in *Glut2*<sup>-/-</sup> mice apart from the significant increase in the kidney uptake (Fig. 4B), possibly as a result of uptake by other GLUTs. In the urinary bladder, there was no significant change in the amount of 2-FDG in *Glut2*<sup>-/-</sup> mice at 60 min compared to wild-type controls (Fig. 4B) (i.e. the filtered load was excreted in both mice). In the liver, there is evidence that 2-FDG uptake is compromised in the absence of GLUT2 in hepatocytes (Fig. 6) (Guillam *et al.* 1998).

The most obvious differences between the distribution of Me-4FDG and 2-FDG in conscious control mice were that Me-4FDG neither entered the brain, nor was excreted into the urinary bladder (Figs 3 and 4). In wild-type, *Sglt1*<sup>-/-</sup> and *Sglt2*<sup>-/-</sup> mice, the amount of Me-4FDG in brain amounted to only 1%ID/g, which is lower than any other region of the body, ~4%ID/g (Fig. 3), and consistent with previous findings that Me-4FDG, [C-11]-methyl-D-glucopyranoside and [F-18]-fluoro-n-alkyl-β-D-glucopyranoside do not normally cross the rat blood–brain barrier (Bormans *et al.* 2003; de Groot *et al.* 2003; Yu *et al.* 2010). Osmotic opening of the blood–brain barrier permits Me-4FDG to enter the brain and accumulate in specific regions, such as the hippocampus and cerebellum (Yu *et al.* 2013). The washout of Me-4FDG from the brain (Fig. 3C) probably represents the clearance of tracer from the brain vascular bed and there were no significant changes in the time course in *Sglt1*<sup>-/-</sup> and *Sglt2*<sup>-/-</sup> animals (Fig. 3C). Negligible amounts of Me-4FDG were excreted into the urinary bladder in control mice, although substantial amounts were excreted in the *Sglt1*<sup>-/-</sup> and *Sglt2*<sup>-/-</sup> mice (Figs 3G and 7).

The results for 4-FDG brain uptake into the brain are consistent with our previous results showing accumulation in brain regions where SGLTs are expressed (Yu *et al.* 2010, 2013). 4-FDG is poorly excreted by the kidney into the urinary bladder relative to 2-FDG 13 vs. 57%ID/g (Figs 4 and 5). Our results for 4-FDG are similar to those reported previously for 6-FDG in the rat (Landau *et al.* 2007) and suggest that 4-FDG and 6-FDG are equally good tracers for PET studies activity because both are substrates for SGLTs and GLUTs. In *Glut2*<sup>-/-</sup> mice, there were no significant changes in the 60 min uptake of 4-FDG

in the brain, heart or skeletal muscle, although there were notable increases in 4-FDG activity in the kidney (Fig. 5B). This demonstrates that GLUT2 is relatively unimportant in glucose uptake into the brain and muscle, although it is required for glucose reabsorption from glomerular filtrate back into the blood (see below).

Overall, the present study confirms that GLUT2 is required for glucose uptake into the liver (Guillam *et al.* 1998) and for glucose reabsorption from glomerular filtrate in the kidney (Guillam *et al.* 1997; Thorens *et al.* 2000; Santer *et al.* 2002). Excretion of 2-FDG into the urinary bladder approaches the filtered load and there is no increase in *Glut2*<sup>-/-</sup> mice. Recall that 2-FDG is not a high-affinity substrate for SGLTs in the apical membrane. GLUT2 plays a minor role, if any, in glucose uptake into brain across the blood–brain barrier, skeletal muscle or heart. A minor caveat is that Me-4FDG uptake into heart is increased in *Sglt1*<sup>-/-</sup> mice (Fig. 3), suggesting a role for SGLTs in heart glucose metabolism. In mice and humans lacking functional GLUT2 transporters, there is no apparent defect in intestinal glucose absorption (Guillam *et al.* 1997; Stumpel *et al.* 2001; Santer *et al.* 2003a).

SGLTs appear to have a relatively minor role in overall glucose utilization in the liver, skeletal muscle, heart and brain, although they are essential for glucose reabsorption in the kidney. In our studies, SGLT1 and SGLT2 appear to be equally important in Me-4FDG reabsorption from the glomerular filtrate. This is somewhat different from the results reported for urinary glucose excretion where there were only 2–3% and 25–35% decreases in reabsorption in *Sglt1*<sup>-/-</sup> and *Sglt2*<sup>-/-</sup> mice (Vallon *et al.* 2010; Vallon, 2011; Gorboulev *et al.* 2012; Powell *et al.* 2013). The differences may be partly explained by the variations in renal glucose excretion seen in the knockout mice (Fig. 5) (Powell *et al.* 2013). In wild-type mice, it is estimated that SGLT2 in the early proximal tubule accounts for the reabsorption of 80% of the filtered glucose (Vallon *et al.* 2010) but, at least in the *Sglt2* knockout animals, the reserve capacity of SGLT1 of the late proximal tubule can salvage 50% or more of the glucose in the absence of SGLT2 (Powell *et al.* 2013). A similar conclusion may be drawn about patients without functional SGLT2 protein where substantial amounts of glucose are reabsorbed (Santer *et al.* 2003b).

Finally, these results raise a question concerning the role of GLUT2 in the reabsorption of glucose in the kidney: Me-4FDG and αMDG are low affinity substrates for GLUT2, yet both are completely absorbed in wild-type mice. How then does Me-4FDG (and MDG) exit from the proximal tubular epithelium into the blood across the basolateral membrane? One possibility is that GLUT2, with a very low affinity for Me-4FDG ( $K_i \sim 100$  mM) (Table 1) is adequate to permit the escape of accumulated Me-4FDG into blood. As supporting evidence, Me-4FDG

is not reabsorbed from the glomerular filtrate in Glut2<sup>-/-</sup> mice (Fig. 7).

## References

- Balen D, Ljubojevic M, Breljak D, Brzica H, Zlender V, Koepsell H & Sabolic I (2008). Revised immunolocalization of the Na<sup>+</sup>-D-glucose cotransporter SGLT1 in rat organs with an improved antibody. *Am J Physiol Cell Physiol* **295**, C475–C489.
- Bormans GM, Van Oosterwyck G, De Groot TJ, Veyhl M, Mortelmans L, Verbruggen AM & Koepsell H (2003). Synthesis and biologic evaluation of (11)c-methyl-d-glucoside, a tracer of the sodium-dependent glucose transporters. *J Nucl Med* **44**, 1075–1081.
- Chen J, Williams S, Ho S, Loraine H, Hagan D, Whaley JM & Feder JN (2010). Quantitative PCR tissue expression profiling of the human SGLT2 gene and related family members. *Diabetes* **1**, 57–92.
- Chow PL, Rannou FR & Chatziioannou AF (2005). Attenuation correction for small animal PET tomographs. *Phys Med Biol* **50**, 1837–1850.
- de Groot TJ, Veyhl M, Terwinghe C, Vanden Bempt V, Dupont P, Mortelmans L, Verbruggen AM, Bormans GM & Koepsell H (2003). Synthesis of 18F-fluoroalkyl-beta-D-glucosides and their evaluation as tracers for sodium-dependent glucose transporters. *J Nucl Med* **44**, 1973–1981.
- Diez-Sampedro A, Wright EM & Hirayama BA (2001). Residue 457 controls sugar binding in the Na(+)/glucose cotransporter. *J Biol Chem* **276**, 49188–49194.
- Ferl GZ, Zhang X, Wu HM, Kreissl MC & Huang SC (2007). Estimation of the 18F-FDG input function in mice by use of dynamic small-animal PET and minimal blood sample data. *J Nucl Med* **48**, 2037–2045.
- Gallagher BM, Fowler JS, Guttererson NI, MacGregor RR, Wan CN & Wolf AP (1978). Metabolic trapping as a principle of radiopharmaceutical design: some factors responsible for the biodistribution of [18F] 2-deoxy-2-fluoro-D-glucose. *J Nucl Med* **19**, 1154–1161.
- Ghezzi C, Hirayama BA, Gorraitz E, Loo DD, Liang Y & Wright EM (2014). SGLT2 inhibitors act from the extracellular surface of the cell membrane. *Physiol Rep* **2**, e12058.
- Gorboulev V, Schurmann A, Vallon V, Kipp H, Jaschke A, Klessen D, Friedrich A, Scherneck S, Rieg T, Cunard R, Veyhl-Wichmann M, Srinivasan A, Balen D, Breljak D, Rexhepaj R, Parker HE, Gribble FM, Reimann F, Lang F, Wiese S, Sabolic I, Sendtner M & Koepsell H (2012). Na<sup>+</sup>-D-glucose cotransporter SGLT1 is pivotal for intestinal glucose absorption and glucose-dependent incretin secretion. *Diabetes* **61**, 187–196.
- Grundy D (2015). Principles and standards for reporting animal experiments in *The Journal of Physiology* and *Experimental Physiology*. *J Physiol* **593**, 2547–2549.
- Guillam MT, Burcelin R & Thorens B (1998). Normal hepatic glucose production in the absence of GLUT2 reveals an alternative pathway for glucose release from hepatocytes. *Proc Natl Acad Sci USA* **95**, 12317–12321.
- Guillam MT, Hummler E, Schaerer E, Yeh JI, Birnbaum MJ, Beermann F, Schmidt A, Deriaz N & Thorens B (1997). Early diabetes and abnormal postnatal pancreatic islet development in mice lacking Glut-2. *Nat Genet* **17**, 327–330.
- Huang SC, Truong D, Wu HM, Chatziioannou AF, Shao W, Wu AM & Phelps ME (2005). An internet-based 'kinetic imaging system' (KIS) for MicroPET. *Mol Imaging Biol* **7**, 330–341.
- Hummel CS, Lu C, Liu J, Ghezzi C, Hirayama BA, Loo DD, Kepe V, Barrio JR & Wright EM (2011). Structural selectivity of human SGLT inhibitors. *Am J Physiol Cell Physiol* **302**, C373–C382.
- Kreissl MC, Stout DB, Wong KP, Wu HM, Caglayan E, Ladno W, Zhang X, Prior JO, Reiners C, Huang SC & Schelbert HR (2011). Influence of dietary state and insulin on myocardial, skeletal muscle and brain [F]-fluorodeoxyglucose kinetics in mice. *EJNMMI Res* **1**, 8.
- Landau BR, Spring-Robinson CL, Muzic RF Jr., Rachdaoui N, Rubin D, Berridge MS, Schumann WC, Chandramouli V, Kern TS & Ismail-Beigi F (2007). 6-Fluoro-6-deoxy-D-glucose as a tracer of glucose transport. *Am J Physiol Endocrinol Metab* **293**, E237–E245.
- Loening AM & Gambhir SS (2003). AMIDE: a free software tool for multimodality medical image analysis. *Mol Imaging* **2**, 131–137.
- Mueckler M & Thorens B (2013). The SLC2 (GLUT) family of membrane transporters. *Mol Aspects Med* **34**, 121–138.
- Nishimura M & Naito S (2005). Tissue-specific mRNA expression profiles of human ATP-binding cassette and solute carrier transporter superfamilies. *Drug Metab Pharmacokinet* **20**, 452–477.
- Phelps ME (2004). *PET Molecular Imaging and Its Biological Applications*. Springer, New York, NY.
- Powell DR, DaCosta CM, Gay J, Ding ZM, Smith M, Greer J, Doree D, Jeter-Jones S, Mseeh F, Rodriguez LA, Harris A, Buhning L, Platt KA, Vogel P, Brommage R, Shadoan MK, Sands AT & Zambrowicz B (2013). Improved glycemic control in mice lacking SglT1 and SglT2. *Am J Physiol Endocrinol Metab* **304**, E117–E130.
- Santer R, Groth S, Kinner M, Dombrowski A, Berry GT, Brodehl J, Leonard JV, Moses S, Norgren S, Skovby F, Schneppenheim R, Steinmann B & Schaub J (2002). The mutation spectrum of the facilitative glucose transporter gene SLC2A2 (GLUT2) in patients with Fanconi-Bickel syndrome. *Hum Genet* **110**, 21–29.
- Santer R, Hillebrand G, Steinmann B & Schaub J (2003a). Intestinal glucose transport: evidence for a membrane traffic-based pathway in humans. *Gastroenterology* **124**, 34–39.
- Santer R, Kinner M, Lassen CL, Schneppenheim R, Eggert P, Bald M, Brodehl J, Daschner M, Ehrlich JH, Kemper M, Li Volti S, Neuhaus T, Skovby F, Swift PG, Schaub J & Klaerke D (2003b). Molecular analysis of the SGLT2 gene in patients with renal glucosuria. *J Am Soc Nephrol* **14**, 2873–2882.
- Scafoglio C, Hirayama BA, Kepe V, Liu J, Ghezzi C, Satyamurthy N, Moatamed NA, Huang J, Koepsell H, Barrio JR & Wright EM (2015). Functional expression of sodium-glucose transporters in cancer. *Proc Natl Acad Sci USA* **112**, E4111–E4119.



- Segel IH (1975). Enzyme kinetics: Behavior and analysis of rapid equilibrium and steady state kinetics. John Wiley & Sons, Inc., New York.
- Stumpel F, Burcelin R, Jungermann K & Thorens B (2001). Normal kinetics of intestinal glucose absorption in the absence of GLUT2: evidence for a transport pathway requiring glucose phosphorylation and transfer into the endoplasmic reticulum. *Proc Natl Acad Sci USA* **98**, 11330–11335.
- Suckow C, Kuntner C, Chow P, Silverman R, Chatziioannou A & Stout D (2009). Multimodality rodent imaging chambers for use under barrier conditions with gas anesthesia. *Mol Imaging Biol* **11**, 100–106.
- Thorens B, Guillam MT, Beermann F, Burcelin R & Jaquet M (2000). Transgenic reexpression of GLUT1 or GLUT2 in pancreatic beta cells rescues GLUT2-null mice from early death and restores normal glucose-stimulated insulin secretion. *J Biol Chem* **275**, 23751–23758.
- Vallon V (2011). Molecular determinants of renal glucose reabsorption. Focus on ‘Glucose transport by human renal Na<sup>+</sup>/D-glucose cotransporters SGLT1 and SGLT2’. *Am J Physiol Cell Physiol* **300**, C6–C8.
- Vallon V, Platt KA, Cunard R, Schroth J, Whaley J, Thomson SC, Koepsell H & Rieg T (2010). SGLT2 mediates glucose reabsorption in the early proximal tubule. *J Am Soc Nephrol* **22**, 104–112.
- Vrhovac I, Balen Erer D, Klessen D, Burger C, Breljak D, Kraus O, Radovic N, Jadrijevic S, Aleksic I, Walles T, Sauvant C, Sabolic I & Koepsell H (2015). Localizations of Na-D-glucose cotransporters SGLT1 and SGLT2 in human kidney and of SGLT1 in human small intestine, liver, lung, and heart. *Pflügers Arch* **467**, 1881–1898.
- Wong KP, Sha W, Zhang X & Huang SC (2011). Effects of administration route, dietary condition, and blood glucose level on kinetics and uptake of 18F-FDG in mice. *J Nucl Med* **52**, 800–807.
- Wong KP, Zhang X & Huang SC (2013). Improved derivation of input function in dynamic mouse [18F]FDG PET using bladder radioactivity kinetics. *Mol Imaging Biol* **15**, 486–496.
- Wright EM (2013). Glucose transport families SLC5 and SLC50. *Mol Aspects Med* **34**, 183–196.
- Wright EM, Barrio JR, Hirayama B & Kepe V (2014). Tracers for monitoring the activity of sodium/glucose cotransporters in health and disease. United States Patent US 8,845,99 B2.
- Wright EM, Loo, DDF & Hirayama BA (2011). Biology of human sodium glucose transporters. *Physiol Rev* **91**, 733–794.
- Wright EM, Martin MG & Turk E (2001). Familial glucose-galactose malabsorption and hereditary renal glycosuria. In *The Metabolic & Molecular Bases of Inherited Disease*, eds Scriver CR, Beaudet AL, Sly WS, Valle D, Childs B, Kinzler KW & Vogelstein B, pp. 4891–4908. McGraw-Hill, New York, NY.
- Yu AS, Hirayama BA, Timbol G, Liu J, Diez-Sampedro A, Kepe V, Satyamurthy N, Huang SC, Wright EM & Barrio JR (2013). Regional distribution of SGLT activity in rat brain in vivo. *Am J Physiol Cell Physiol* **304**, C240–C247.
- Yu AS, Hirayama BA, Timbol G, Liu, J, Basarah E, Kepe V, Satyamurthy N, Wright EM, Huang S-C & Barrio JR (2010). Functional expression of SGLTs in rat brain. *Am J Physiol Cell Physiol* **299**, C1277–C1284.

## Additional information

### Competing interests

The authors declare that they have no competing interests.

### Author contributions

MS-R, EMW and JRB were responsible for the study concept and design. MS-R, BAH, CG and JL were responsible for the acquisition of data. MS-R, BAH, JL, VK, AY, HK, S-CH, DRP and EMW were responsible for data analysis. JL and VK were responsible for chemical design, synthesis and analysis. MS-R, JRB and EMW were responsible for manuscript preparation and revision. EMW, JRB, M-SR, DRP, S-HH and HK were responsible for interpretation of the data. All authors have approved the final version of the manuscript and agree to be accountable for all aspects of the work. All persons designated as authors qualify for authorship, and all those who qualify for authorship are listed.

### Funding

This work was supported by grants from the National Institutes of Health (Grants RO1-DK19567 (Wright) and RO1-DK077133 (Wright) and the Elizabeth and Thomas Plott Endowed Chair in Gerontology (Barrio). Additional funding was provided by a Pilot and Feasibility Grant from the UCLA Digestive Diseases Research Centre, and the Mitzi and William Bland Pilot Research Grant from the Society of Nuclear Medicine (Sala-Rabanal).

### Acknowledgements

Glut2<sup>-/-</sup> mice were provided by Colin Nichols (Washington University in Saint Louis, MO, USA). SglT1<sup>-/-</sup> mice were provided by Volker Vallon (University of California San Diego, CA, USA). SglT2<sup>-/-</sup> mice were obtained from Lexicon Pharmaceuticals, Inc., The Woodlands, TX, USA. Waldemar Ladno is greatly appreciated for his skill, patience and instruction on all aspects of mouse microPET determinations. The authors thank William F. Borschel (Washington University School of Medicine) for assistance with two-way ANOVA.

### **Translational perspective**

The introduction of 2-FDG PET imaging some 30 years ago revolutionized our ability to monitor glucose metabolism in human subjects. This led to new perspectives in the human physiology of the brain and heart, and novel ways to identify, stage cancers and follow cancer therapy. Unfortunately, 2-FDG PET did not report on the activity of the second class of glucose transporters, the SGLTs. Our new specific imaging probe for SGLTs promises to provide novel insights into the human physiology of SGLTs, and diseases such as diabetes and cancer. SGLT2 inhibitors have been approved for the treatment of type 2 diabetes mellitus, and SGLT2 has been shown to be expressed in pancreatic and prostate cancers. We envisage that SGLT PET imaging will prove to be a powerful tool in the development of new drugs for treating diabetes and cancer, and for determining their efficacy and safely.